Applied Catalysis A: General 378 (2010) 151–159

Contents lists available at ScienceDirect

Applied Catalysis A: General

journal homepage: www.elsevier.com/locate/apcata

Synthesis, structure and catalytic activity of nano-structured Sr–Ru–O type perovskite for hydrogen production

Ahmed Galal *, Soher A. Darwish, Nada F. Atta, Shimaa M. Ali, Ahmed A. Abd El Fatah

Department of Chemistry, Faculty of Science, University of Cairo, 1 Gama Al Kahira Street, Postal Code 12613 Giza, Egypt

ARTICLE INFO

Article history:
Received 22 September 2009
Received in revised form 7 February 2010
Accepted 10 February 2010
Available online 18 February 2010

Keywords:
Perovskites
Microwave irradiation processing
Nano-particles
Electrocatalyst
Hydrogen evolution reaction
XRD
SEM
Tafel
Impedance

ABSTRACT

$SrRuO_3$ perovskite was synthesized by three different methods, namely microwave assistant-citrate, citrate-nitrate and coprecipitation. The resulting perovskite structure was characterized by XRD and SEM measurements. The electrocatalytic activity of the perovskites was examined toward hydrogen evolution reaction (HER) by Tafel linear polarization and impedance techniques. $SrRuO_3$ prepared by the microwave method showed superior catalytic activity compared to those synthesized by other chemical methods. The values of the exchange current densities are -14.7×10^2, -52.2 and -13.1 μA cm^{-2} for $SrRuO_3$ prepared by the microwave, citrate-nitrate and coprecipitation methods, respectively. The reaction order and the activation energy for each catalyst were determined. The calculated values of the activation energy are in good agreement with the trend for catalytic activity. Both Tafel and impedance data showed that the Volmer step is the rate-determining step. The particle size calculated from XRD measurements are 30.7, 41.5 and 42.2 nm for the perovskites prepared by microwave assistant-citrate, citrate-nitrate and coprecipitation methods, respectively.

1. Introduction

The conception of microwave sintering was first reported by Tinga and Voss [1] in 1960s and has been intensively investigated since the mid of 1970s by Berteaud and Badet [2]. The advantages of microwave irradiation processing (MIP) have been summarized as follows: (i) rapid reaction velocity, (ii) uniform heating and (iii) clean and energy efficient. Since its development, nanoscience affected the progress in various scientific domains including catalysis [3]. Thus, multifarious soft-chemical and self-assembly methods have been brought into the preparation of perovskites in the past few decades to increasingly precise control of the variables affecting physicochemical properties. However, most of these methods need both high calcination temperature (>700 °C) and long time (>3 h) for pretreatment or sintering. MIP is suggested to be the most potential method to reduce the aforementioned disadvantages. During the past years, many perovskites such as $GaAlO_3$, $LaCrO_3$, etc., have been reported to be synthesized by MIP for their ferro-electricity, superconductivity, high-temperature ionic conductivity, or a variety of magnetic ordering, etc. [4–6]. It was reported that smaller grain size and more rapid lattice diffusion would be formed in microwave route than in other wet chemical processes [7], which might enhance the lattice oxygen mobility in catalysis process. Nevertheless, none of them focused on the catalytic activity of perovskites. Ruthenium based perovskites show good thermal stability and tailored catalytic properties, which renders them attractive for high-temperature catalytic applications. It is well established that the synthesis method plays an important role in the catalytic performance of different materials. The different synthesis methods generate structural, surface and textural changes in the properties of the materials, influencing their catalytic behavior [8]. The improved synthesis of metal ruthenate is therefore a key issue for most of their applications.

On the other hand, hydrogen evolution reaction (HER) is an attractive reaction that illustrates the importance of research in the field of renewable energy. The electrocatalysis in the HER is one of the most important subjects in the field of electrochemistry. The ability of a given metal to catalyze the HER is usually measured by the exchange current density. Three properties play an important role in selecting catalytically active materials for hydrogen evolution: (a) an actual intrinsic electrocatalytic effect of the material, (b) a large active surface area per unit volume ratio, both of which are directly related to the overpotential used to operate the electrolyzer at significant current densities, and (c) catalyst stability [9]. Thus, from an electrochemical point of view, the

* Corresponding author. Tel.: +20 0235676561; fax: +20 0235727556.
E-mail addresses: galalh@sti.sci.eg, galalah1@yahoo.com (A. Galal).

0926-860X/$ – see front matter © 2010 Elsevier B.V. All rights reserved.
doi:10.1016/j.apcata.2010.02.015

problem to be tackled in order to decrease the cost of electrolytic hydrogen is the reduction of overpotential of the process. The desired decrease in overpotential can be achieved by choosing highly catalytically active electrode materials, or by increasing the active surface area of the electrode. The intrinsic activity depends on the density of active site on the surface, which is controlled by the electronic structure of the material.

In this work, $SrRuO_3$ was prepared by the microwave assistant-citrate, citrate-nitrate and coprecipitation methods. The influence of the synthesis method on the particle size, surface morphology and the catalytic properties toward HER was described by XRD, SEM and Tafel linear polarization and impedance. In addition the activation energy, the reaction order and the reaction mechanism have been investigated.

2. Experimental

2.1. Chemicals and reagents

Ruthenium chloride hydrate (Fluka, purum, 41% Ru), ruthenium nitrosoyl nitrate (Strem Chemicals, 1.5% Ru), strontium nitrate, citric acid, nitric acid, sulfuric acid, potassium hydroxide, ammonia, (Aldrich), graphite powder (Sigma–Aldrich, <20 μm, synthetic) and Paraffin oil (Fluka) were used as received without further purification. All solutions were prepared using double distilled water. All measurements were made in oxygen-free solution, which was achieved by continuous purging of the cell electrolyte with nitrogen gas (99.999% pure).

2.2. Catalysts preparation

2.2.1. The citrate-nitrate method

Stoichiometric amounts of $Sr(NO_3)_3$ and $RuCl_3{\cdot}xH_2O$ were weighed, dissolved in distilled water and stirred for 5 min. To this aqueous solution, a sufficient amount of citric acid was added so that the molar ratio of citric acid to total metal ions is 1:1. The solution was stirred thoroughly to obtain a uniform mixing. Ammonia was added to adjust the pH of the solution at 8. The solution was heated on a hot plate to about 250 °C. The precursor complex was dehydrated leading to smooth deflation foam. The foam was ignited giving a voluminous black fluffy powder. Then a ceramic nano-oxide was obtained by calcinations for 5 h at 600 °C.

2.2.2. Coprecipitation

Weighed amounts of $Sr(NO_3)_2$ and $RuCl_3{\cdot}xH_2O$ were dissolved in distilled water and stirred for 5 min with a magnetic stirrer. Aqueous 3 M KOH solution was added with constant stirring until the pH of the reaction medium reached 13, a black precipitate immediately formed. The solution was stirred for 1 h at room temperature, then allowed to stand for several hours, and washed with distilled water several times in order to remove potassium ions. Then the precipitate was filtrated, dried in an oven at 70 °C, grounded in a mortar for 10 min and finally calcinated at 600 °C in a muffle furnace for 5 h to obtain nano-crystalline $SrRuO_3$.

2.2.3. The microwave assistant-citrate method

Mixed citrate complex was first prepared as indicated in Section 2.2.1 from the nitrate precursors then, placed in a conventional microwave oven and the reaction was performed under ambient air for 30 min. The microwave was operated in 30-s cycles (20 s on, 10 s off). The precursor complex dehydrated and became more viscous with time producing a dark gel mass. The gel was ignited which gave a voluminous fluffy powder. A ceramic nano-$SrRuO_3$ was obtained by calcination at 600 °C for 5 h.

All electrochemical measurements: the dc polarization and the electrochemical impedance spectroscopy (EIS), were carried out in aqueous acid 0.1 M H_2SO_4. Polarization measurements of hydrogen evolution were carried out by first stabilization at open-circuit potential (OCP) until a steady-state value was obtained (usually after about 30 min), then conditioning the electrode at −0.2 V for 10 min and at −0.3 V for 5 min. Then, a linear polarization measurement was conducted starting from −0.3 to −0.6 V, at a scan rate of 1 mV s^{-1}. The dc polarization measurement was followed by a set of electrochemical impedance spectroscopy measurements at selected overpotentials.

2.3. Electrochemical cell and electrode preparation

A standard three-electrode, one compartment cell was used in all experiments. The counter electrode was a large surface area platinum electrode. The reference electrode was commercially available saturated silver/silver chloride electrode. The working electrode was carbon paste electrode (CpE) (d = 0.63 cm), the unmodified CpE was prepared as follows: 0.125 g of reagent grade graphite powder was washed with acetone, dried then was mixed with 45 μL of paraffin oil. To modify the CpE, the graphite powder was mixed with the modifier in a given composition ratio. Both unmodified and modified carbon pastes were packed into a Teflon holder that was surface reset at the end. Electrical contact to the paste was established via a thin copper rod passed through the Teflon holder. The fresh surfaces were obtained by polishing the electrodes on a clean fine-grade polishing paper until they showed a smooth and shiny appearance prior to every measurement.

2.4. Apparatus and methods

Electrochemical measurements were performed using a Gamry-750 system and a lock-in-amplifier that are connected to a personal computer. The scanning electron microscopy analysis was achieved by using JEOL JSM-6360 LA and Philips XL 30. X-ray diffraction analysis was obtained using Shimadzu XRD-700. Surface area measurements were achieved using Autosorb-6B surface area and pore size analyzer.

3. Results and discussion

3.1. XRD and surface characterization

Strontium ruthenium mixed oxide, $SrRuO_3$ was prepared by microwave assistant-citrate, citrate-nitrate and coprecipitation methods. The compositions prepared were characterized by X-ray powder diffractograms. Fig. 1 shows the XRD of $SrRuO_3$ prepared by (A) microwave assistant-citrate, (B) citrate-nitrate, (C) and coprecipitation methods, respectively. The major diffraction peak (2 0 0) of the as-synthesized powders was matched with the theoretical one. Because of the nano-structured samples, XRD patterns were broad especially that of the sample prepared via the microwave route. The results suggested successful incorporation of Ru^{4+} at the Sr^{2+} cations sites confirming the formation of the orthorhombic perovskite phase of $SrRuO_3$. The XRD also revealed minor peaks ascribable to RuO_2 as indicated in Fig. 1. The XRD patterns of the prepared oxides show mixed polycrystalline diffraction peaks of the RuO_2 (rutile) phase with distinguished peaks of (1 0 1), (1 1 0) and (2 0 0) (corresponding to PDF 43-1027) and diffraction of crystalline $SrRuO_3$ perovskite of (1 0 1), (1 1 1), (1 2 1), (1 2 3) and (3 2 1) at 2θ = 22.00°, 25.50°, 32.50°, 67.50° and 58.0°, respectively (corresponding to JCPDS 43-0472). The crystalline characters of rutile RuO_2 phase and perovskite $SrRuO_3$ phase are more emphasized in the case of using the microwave assistant-citrate and coprecipitation methods when using the same calcinations temperatures and durations.

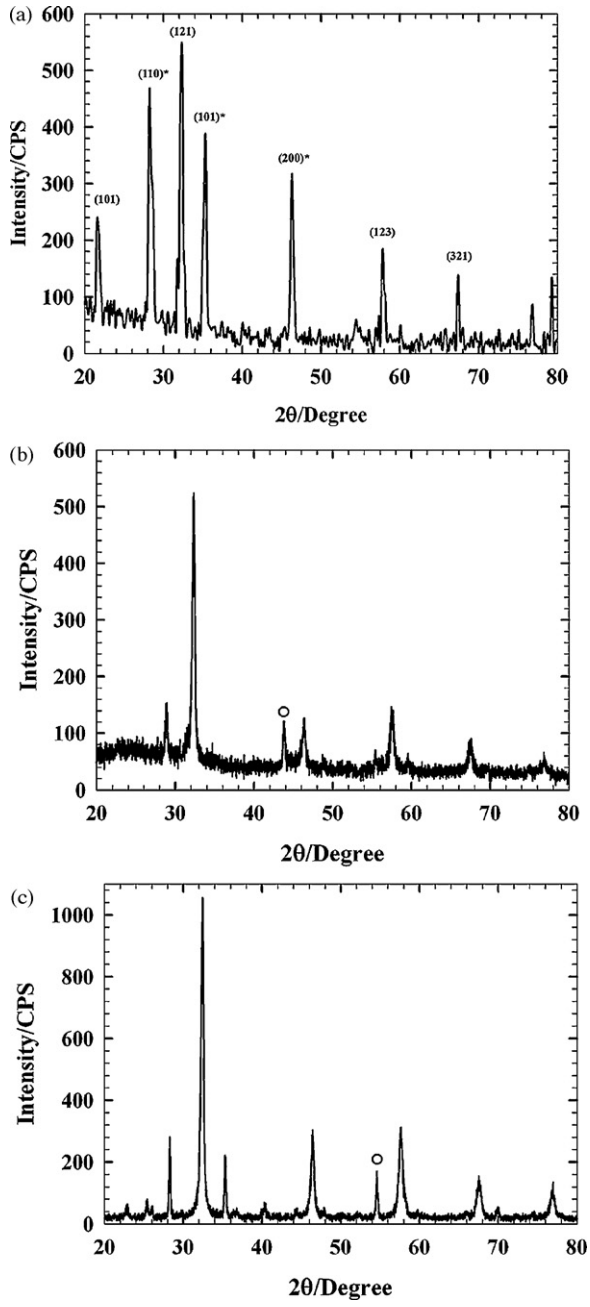

Fig. 1. XRD patterns of $SrRuO_3$ prepared by (A) microwave assistant-citrate, (B) citrate-nitrate, (C) and coprecipitation methods (○ secondary phase, RuO_2). Miller indices (*h*, *l*, *k*) are showed.

In addition to the phase identification, some important structural parameters were calculated from XRD data such as, particle size (from Scherrer equation), lattice parameters, lattice volume and theoretical density [10]. These parameters were listed in Table 1 and found to be in good agreement with those for standard samples (JCPDS card number 25-912). It can be noticed that the synthesis method affects both the particle size and the lattice parameters. The microwave synthesis provided the smallest particle size over the citrate-nitrate and coprecipitation which can be also observed from the SEM images.

The morphology of the prepared perovskites was studied by SEM. The orthorhombic perovskite phase of $SrRuO_3$ was clearly identified from the SEM image of the sample prepared by the microwave method, shown in Fig. 2A. Thus, the microwave route provided best method that resulted in the enhancement of the grain growth in terms of number of particles with expected geometrical structure. Fig. 2B–D shows a comparison between the SEM images of $SrRuO_3$ prepared by the three different methods (a) microwave assistant-citrate, (b) citrate-nitrate, (c) and coprecipitation methods. It can be concluded that the synthesis method affect the morphology and the particle size of the prepared perovskites, the smallest particle size and the highest porosity can be obtained through the microwave route. Samples prepared by citrate-nitrate and coprecipitation was composed of agglomerations of nearly spherical grains, smaller agglomerations and more compact surface were observed in case of citrate-nitrate method. For a film 320 nm thick the roughness factor is 24 nm.

3.2. Investigation of the catalytic activity toward HER by dc-Tafel linear polarization

In order to investigate the electrocatalytic activity of the prepared perovskites toward hydrogen evolution reaction (HER), Tafel linear polarization measurements were performed and the corresponding electrochemical parameters (Tafel slope, exchange current density and transfer coefficient) were derived from the data. Fig. 3 shows a set of Tafel lines recorded in 0.1 M H_2SO_4 in the potential region of hydrogen evolution for carbon paste electrodes modified with 10% (w/w, %) $SrRuO_3$ prepared by: microwave assistant-citrate method, citrate-nitrate method, and coprecipitation, together with unmodified carbon paste electrode. Fig. 3 shows that the presence of the perovskite modifier resulted in increase in the electrocatalytic activity toward HER by about 100 times. The carbon paste electrodes modified with the perovskite catalysts display two potential regions related to HER. At low overpotentials, the curves are characterized by a well-defined Tafel behavior, while at higher overpotentials; a significant deviation from Tafel behavior was recorded. The existence of two Tafel regions (change in Tafel slope) has already been reported in literature [11] for similar HER electrocatalytic materials and a number of explanations have been given. Thus, a change in HER mechanism has been

Table 1
Structural parameters calculated from XRD data.

	Crystal structure	Surface area, $m^2 g^{-1}$	Average particle size, nm	Lattice parameters, Å	Lattice volume, $Å^3$	Theoretical density, g/cm^3
Standard	Orthorhombic			*a* = 5.56 *b* = 5.55 *c* = 7.86	242.54	6.48
Microwave	Orthorhombic	232.60	30.7	*a* = 5.68 *b* = 5.43 *c* = 7.82	240.99	6.52
Sol-combustion	Orthorhombic	90.25	41.46	*a* = 5.54 *b* = 5.56 *c* = 7.80	240.33	6.54
Coprecipitation	Orthorhombic	71.17	42.17	*a* = 5.71 *b* = 5.42 *c* = 7.77	240.38	6.54

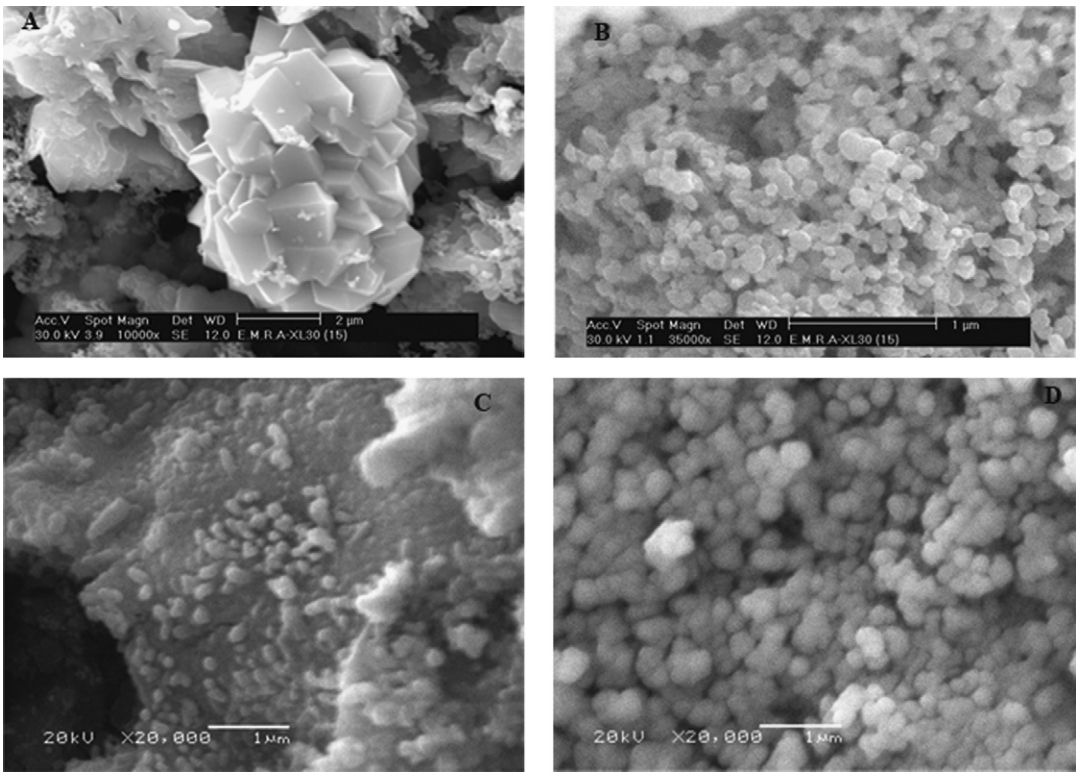

Fig. 2. SEM micrographs of $SrRuO_3$ prepared (A) microwave assistant-citrate, with a magnification of 10,000 times, (B) microwave assistant-citrate, with a magnification of 35,000 times, (C) citrate-nitrate and (D) coprecipitation methods, with a magnification of 20,000 times.

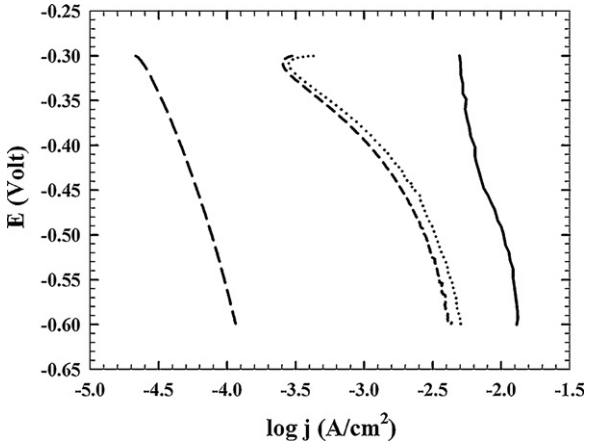

Fig. 3. Linear Tafel polarization curves for the HER recorded on CpE modified with 10% (w/w, %) $SrRuO_3$ prepared by (—) microwave assistant-citrate, (···) citrate-nitrate, (- - -) and coprecipitation methods in 0.1 M H_2SO_4. The long-dashed line (– –) represents a response of unmodified CPE; Scan rate = 1 mV s^{-1}.

suggested as one possible explanation, which can be attributed to the depletion of the *d*-electron density at the Fermi level of the perovskite by adsorbed hydrogen [12] which remained partially uncompensated at lower overpotentials. Mass-transport limitations through narrow pores on the catalyst surface [13] or a decrease in the active surface area [14–16] have also been suggested as possible reason for the observed diffusion-like shape of the Tafel lines.

By considering the Tafel region, it is clear that the HER on carbon paste electrode modified with the catalyst is a kinetically controlled reaction described by the Tafel equation. The values of Tafel slope, exchange current density, and transfer coefficient calculated for $SrRuO_3$ prepared by: microwave assistant-citrate, citrate-nitrate and, coprecipitation methods are listed in Table 2.

According to the general HER mechanism in acidic media [17–19], the Tafel slope values indicate that the Volmer reaction step, i.e. adsorption of hydrogen on the catalyst is the rate-determining step. It could also be noticed that the Tafel slope and transfer coefficient values deviated from the theoretical values 116 mV $decade^{-1}$ and 0.5, respectively [17–19]. This phenomenon has already been reported in the literature [17] and has been explained as a characteristic feature for oxide catalysts. Note that for the Volmer step the symmetry factor, β, is equal to the transfer coefficient, α, while for the Heyrovsky step, i.e. desorption of adsorbed hydrogen to form molecular hydrogen the transfer coefficient α is equal $1+\beta$ [17,20]. Considering the exchange current density values presented in Table 2, which is directly proportional to the reaction rate at equilibrium, one can conclude that microwave method offered the best preparation route for the

Table 2
HER kinetics parameters (the values of Tafel slope, exchange current density, transfer coefficient, overpotential measured at a current density of 1 mA cm^{-2} and current density at a fixed overpotential of −300 mV) obtained by analysis of Linear Tafel polarization curves for $SrRuO_3$ prepared by microwave assistant-citrate, citrate-nitrate and, coprecipitation methods.

Catalyst	*B*, mV dec^{-1}	j_o, μA cm^{-2}	α	*J*, μA cm^{-2} at −300 mV	η, mV at mA cm^{-2}
$SrRuO_3$ (microwave)	835.9	−1465.0	0.071	−5326.0	−60.8
$SrRuO_3$ (sol-combustion)	252.3	−52.2	0.234	−425.5	−383.0
$SrRuO_3$ (coprecipitation)	219.5	−13.1	0.269	−298.0	−394.0

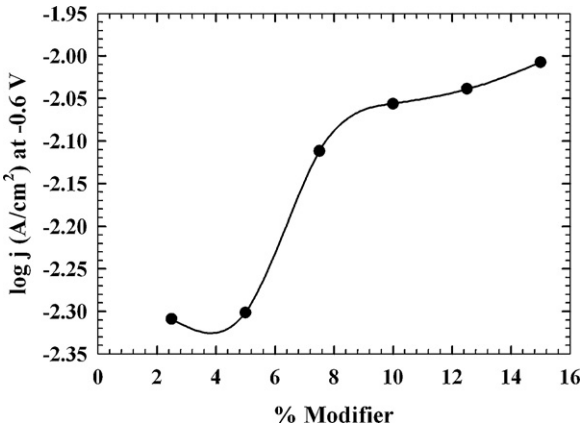

Fig. 4. Typical plot of log j (A cm^{-2}) at −0.6 V (saturated Ag/AgCl) versus the percentage of modifier ($SrRuO_3$ prepared by coprecipitation).

most efficient catalyst over coprecipitation and citrate-nitrate methods. However, although a value of exchange current density is frequently used for the characterization of electrocatalytic activity, it has been reported that values of Tafel slope and transfer coefficient in the low overpotential region (Tafel region) are as or even more important than a favorable exchange current density value [21]. This is due to the fact that the HER does not occur at a reversible potential (i.e. zero overpotential), but certain overpotential is required for the reaction to proceed at a measurable rate. Hence, in order to compare the electrocatalytic activity of the catalysts prepared by different methods at the conditions relevant for the operation of hydrogen generator, one can fix current density (i.e. hydrogen production rate) and compare the resulting overpotentials required to reach the given current density value. This would give an indication of the amount of energy (overpotential) that should be invested to produce a specified amount of hydrogen (since the current is, through the Faraday law, directly related to the amount of the produced hydrogen). Overpotential values for each catalyst, measured at current density of 1 mA cm^{-2} are presented in Table 2. Again, $SrRuO_3$ prepared via the microwave route required the lowest energy (overpotential) for the given hydrogen production rate, −60.8 mV, while that prepared by citrate-nitrate and coprecipitation methods required considerably larger energy inputs, ca. −383 and −394 mV, respectively. This trend was the same as that found in case of using the exchange current density values as a measure to compare the electrocatalytic activity of the catalysts prepared by different methods. Another common way of comparing the electrocatalytic activity of HER electrocatalysts is to fix the overpotential (energy input) and then compares the resulting current density values, i.e. the amount of hydrogen that would be produced by each catalyst. The results for overpotential of −300 mV were presented in Table 2. Similar trend is observed as that obtained in case of the exchange current density and at a fixed current density; $SrRuO_3$ prepared by the microwave synthesis yielded the best electrocatalytic activity. Thus, although the same catalytic material was prepared, $SrRuO_3$, the synthesis method affected greatly the electrocatalytic activity because it affected the morphology, surface area, and particle size of the prepared catalyst. In conclusion, among the different synthetic methods, citrate-nitrate method offered a better route for preparing highly catalytic materials over coprecipitation and this was attributed to the better formed perovskite crystals by the citrate method. Furthermore, highly homogeneous and crystalline oxide with the smallest particle size and largest surface area obtained by the microwave assistant-citrate method showed excellent catalytic activity, among the prepared catalysts by different methods in the present work.

3.3. The effect of catalyst loading in carbon paste electrode

The dependence of the cathodic current response of HER on the catalyst loading in the carbon paste electrode was studied. The current response increased with increasing the catalyst loading because of the increased number of active sites responsible for the catalytic activity. However, further loading of the modifier resulted in a current decrease due to the increased resistance of the modifier [22,23]. This was not shown in case of $SrRuO_3$; as shown in Fig. 4 the current response increased sharply with increasing the catalyst loading till a catalyst percentage of 10% (w/w, %) is reached then the current response was almost constant (slightly increased) as $SrRuO_3$ has a considerable electrical conductivity [24]. The resistivity cited in literature is as low as 275 μΩ cm [[25], and references therein]. Therefore, the suitable catalyst percentage to be used throughout this study is 10% (w/w, %).

3.4. Order of reaction with respect to H^+

The order of the reaction with respect to H^+ was determined at constant ionic strength of the solution by varying the H_2SO_4 concentration keeping the ionic strength constant with Na_2SO_4. Only one dc polarization measurement was taken at each H_2SO_4 concentration by the same procedure mentioned in Section 2. Fig. 5A shows a set of Tafel lines recorded in x M H_2SO_4 (x = 0.05,

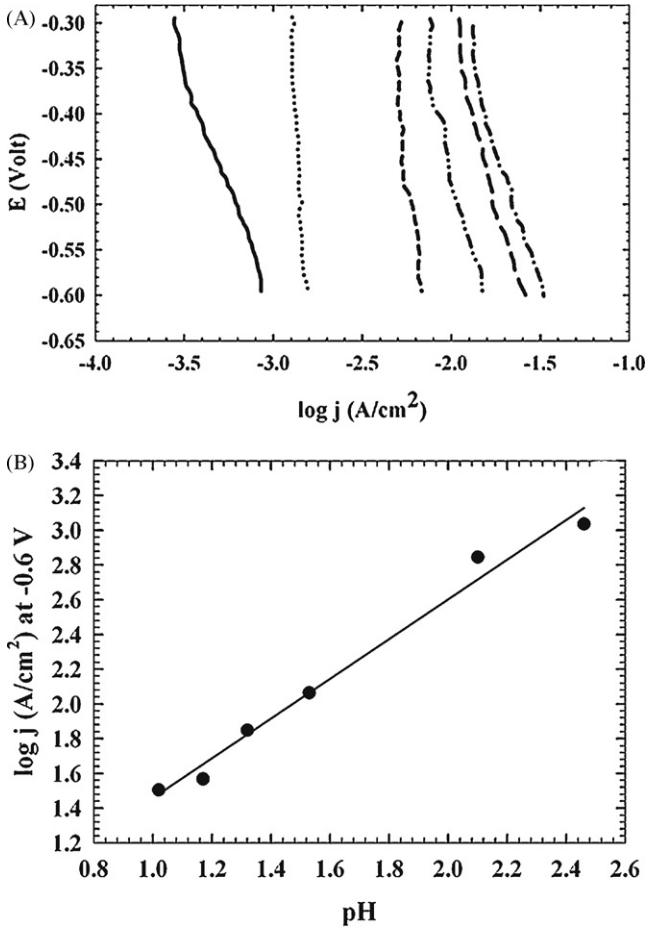

Fig. 5. (A) Linear Tafel polarization curves for the HER recorded on CpE modified with 10% (w/w, %) $SrRuO_3$ prepared by microwave assistant-citrate method in x M H_2SO_4; x = 0.05 (—), 0.1 M (· · ·), 0.2 M (- - -), 0.3 M (- · · -), 0.4 M (– · –) and 0.5 M (– · · –) at room temperatures, scan rate = 1 mV s^{-1}. (B) Typical plot of log j (A cm^{-2}) at −0.6 V (saturated Ag/AgCl) versus pH for the determination of the reaction order for CPE modified with 10% (w/w, %) $SrRuO_3$ prepared by microwave assistant-citrate method, slope = 1.14.

0.1, 0.2, 0.3, 0.4, and 0.5 M) in the potential region of hydrogen evolution at carbon paste electrode modified with 10% (w/w, %) $SrRuO_3$ prepared by microwave assistant-citrate method (data for $SrRuO_3$ prepared by citrate-nitrate and coprecipitation methods are not shown). Fig. 5B represents the dependence of the cathodic current of HER on the H^+ ion concentration. The reaction order can be accurately determined since the points gather closely around a straight line. The reaction order values of $SrRuO_3$ prepared by microwave assistant-citrate method, citrate-nitrate method, and coprecipitation are 1.14, 0.98, and 0.88, respectively. The fractional reaction order was expected for HER catalyzed by oxide catalysts [26].

3.5. Activation energy

In order to evaluate the temperature effect on the kinetics of the HER for the catalysts prepared by different methods, dc linear polarization (Tafel) measurements were done for a wide temperature range, from 298 to 338 K. Fig. 6A shows a set of Tafel lines recorded on carbon paste electrode modified with 10% (w/w, %) $SrRuO_3$ prepared by microwave assistant-citrate method at various temperatures. With an increase in temperature, the current density at a fixed overpotential also increased. Fig. 6B demonstrates that this increase was linear in a semi-logarithmic plot, which is in accordance with the Arrhenius equation:

$$\log j_0 = \frac{-2.303E_a}{RT + \log A} \quad (1)$$

where A (A cm^{-2}) is the pre-exponential factor and E_a (J mol^{-1}) is the apparent activation energy. Thus, from the slope of the line, the apparent activation energy value could be calculated. The activation energy values for $SrRuO_3$ prepared by microwave assistant-citrate, citrate-nitrate, and coprecipitation methods, respectively, were 6.67, 49.45, and, 86.32 kJ mol^{-1}, respectively. This trend agreed well with the trend concluded from Tafel measurements; $SrRuO_3$ synthesized via the microwave route offered the highest catalytic activity. The calculated activation energy values for $SrRuO_3$ catalysts prepared by different methods were less than that calculated for Ru catalyst [27]. This can be explained by the fact that Ru in the perovskite structure is highly dispersed and stabilized, in other words, Ru^{3+} cations are homogeneously distributed in the inert perovskite matrix during the reaction (the matrix effect of the stable perovskite crystal structure) [28].

The corresponding electrochemical parameters, Tafel slopes and transfer coefficients together with the exchange current densities at various temperatures are depicted in Table 3. The Tafel slope is usually considered to increase proportionally with temperature according to the relation $b = RT/\alpha F$ based on the assumption of a temperature-independent transfer coefficient α [29]. However, in this work, the Tafel slope-temperature relations did not show the expected behavior exactly and a more complicated relation between the Tafel slope and temperature should be considered. According to Conway [29], for electrochemical reactions including the HER on different electrode materials, the transfer coefficient α is supposed to vary linearly with temperature:

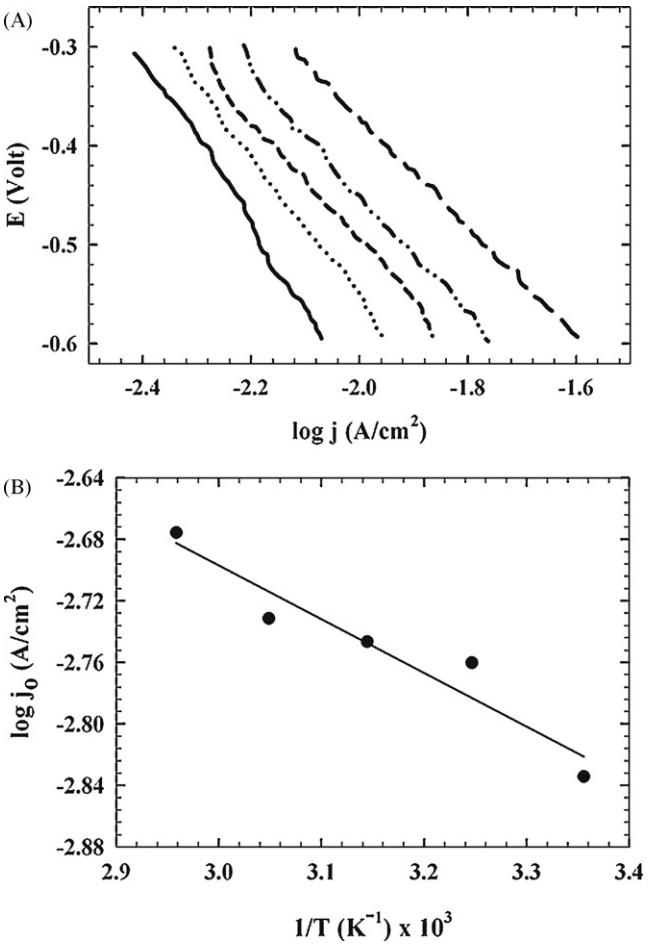

Fig. 6. (A) Linear Tafel polarization curves for the HER recorded on CpE modified with 10% (w/w, %) $SrRuO_3$ prepared by microwave assistant-citrate method in 0.1 M H_2SO_4 at various temperatures: 298 K (—), 308 K (· · ·), 318 K (- - -), 328 K (- · · -), 338 K (– · –); scan rate = 1 mV s^{-1}. (B) The Arrhenius plot for the HER on CpE modified with 10% (w/w, %) $SrRuO_3$ prepared by microwave assistant-citrate method in 0.1 M H_2SO_4.

$$\alpha = \alpha_H + \alpha_S T \quad (2)$$

where α_H and α_S are enthalpy and entropy components. The results showed that the transfer coefficient for HER on carbon paste electrode modified with $SrRuO_3$, prepared by microwave assistant-citrate method increased with temperature. On the other hand, the transfer coefficients for $SrRuO_3$ prepared by citrate-nitrate and coprecipitation methods decrease with temperature. The last behavior has already been reported in literature for HER on Ni electrode [30]. The values of α_H and α_S obtained for the catalysts

Table 3
HER kinetics parameters (the values of Tafel slope, exchange current density and transfer coefficient) obtained by analysis of Linear Tafel polarization curves at various temperatures for $SrRuO_3$ prepared by microwave assistant-citrate, citrate-nitrate and, coprecipitation methods.

T, K	$SrRuO_3$ (microwave)			$SrRuO_3$ (sol-combustion)			$SrRuO_3$ (coprecipitation)		
	b, mV dec^{-1}	j_o, μA cm^{-2}	α	b, mV dec^{-1}	j_o, μA cm^{-2}	α	b, mV dec^{-1}	j_o, μA cm^{-2}	α
298	835.9	−1464.9	0.071	252.3	−52.5	0.234	219.5	−13.1	0.269
308	730.6	−1736.8	0.083	293.4	−77.8	0.208	257.9	−42.6	0.236
318	620.3	−1792.1	0.102	293.9	−117.8	0.214	334.2	−161.8	0.188
328	613.7	−1855.8	0.106	354.5	−284.1	0.183	326.9	−309.5	0.199
338	550.6	−2110.4	0.122	389.3	−540.1	0.172	410.2	−840.8	0.163

Table 4
The values of α_H and α_S obtained for $SrRuO_3$ prepared by microwave assistant-citrate, citrate-nitrate and, coprecipitation methods on the basis of Eq. (2).

Catalyst	α_H	α_S, K^{-1}
$SrRuO_3$ (microwave)	−0.30	1.24×10^{-3}
$SrRuO_3$ (sol-combustion)	0.67	1.48×10^{-3}
$SrRuO_3$ (coprecipitation)	1.00	-2.49×10^{-3}

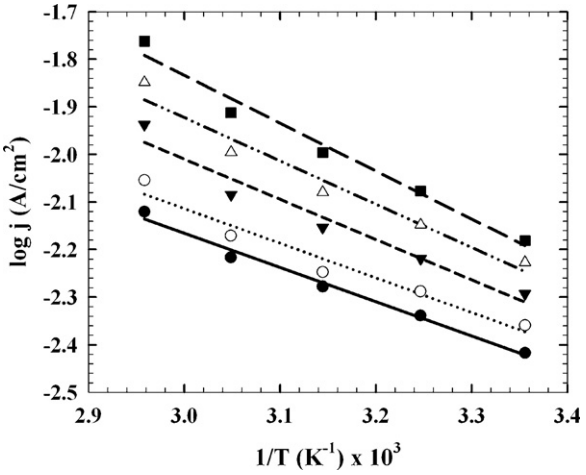

Fig. 7. The Arrhenius plot for the HER on CpE modified with 10% (w/w, %) $SrRuO_3$ prepared by microwave assistant-citrate method in 0.1 M H_2SO_4 at different potentials: −300 mV (●), −350 mV (○), −400 mV (▼), −450 mV (△), −500 mV (■).

prepared by different methods on the basis of this relationship are listed in Table 4.

Fig. 7 represents the Arrhenius plot for the HER on carbon paste electrode modified with $SrRuO_3$ prepared by microwave assistant-citrate. The current densities at different potentials are obtained from the polarization curves measured at different temperatures ranging from 298 to 338 K. The activation energies for the HER are calculated at different potentials. Table 5 list the apparent activation energies values calculated at several selected over-potentials. The values obtained at zero overpotential (equilibrium) are very close to those usually postulated for HER occurring through the Heyrovsky mechanism [31]. Savadogo and coworker [31] obtained values ranging from 36 to 56 kJ mol^{-1} on Pt–Co supported on carbon at zero overpotential, while Giz et al. [32] reported a value of 39 kJ mol^{-1} on NiZn. A higher value (62 kJ mol^{-1}) was reported on NiFeZn [33].

The linear potential dependency of the activation energies has a slope of $\alpha_H F$ [34]. The values of α_H for $SrRuO_3$ prepared by microwave assistant-citrate, citrate-nitrate, and coprecipitation methods are presented in Table 6 and found to be close to those derived from the temperature dependency of transfer coefficient. Also, the intercepts of the linear relations of E_a versus η were presented in Table 6. These intercepts represented the potential-independent part of the activation energy and were in the same range as those reported in literatures [35,36].

Table 6
The slopes, intercepts of the linear relations of E_a versus η, together with the calculated values of α_H for $SrRuO_3$ prepared by microwave assistant-citrate, citrate-nitrate and, coprecipitation methods.

Catalyst	Slope, C mol^{-1}	Intercept, kJ mol^{-1}	α_H
$SrRuO_3$ (microwave)	-2.88×10^4	4.53	−0.30
$SrRuO_3$ (sol-combustion)	7.88×10^4	64.33	0.82
$SrRuO_3$ (coprecipitation)	8.16×10^4	77.06	0.85

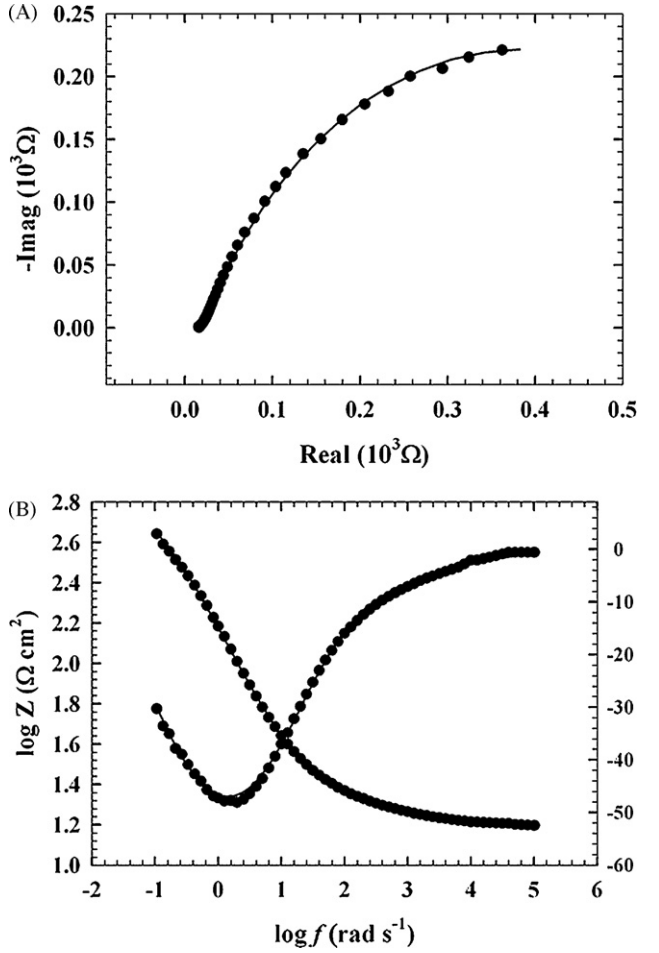

Fig. 8. Bode (A) and (B) Nyquist plots showing An EIS response of CpE modified with 10% (w/w, %) $SrRuO_3$ prepared by microwave assistant-citrate method in 0.1 M H_2SO_4 at ovepotential −0.1 V, symbols are experimental and solid lines are modeled data, respectively.

3.6. Electrochemical impedance spectroscopy

To ensure a complete characterization of the electrode/electrolyte interface and corresponding processes, EIS measurements were performed over a frequency range from 100 kHz to 10 mHz at selected overpotentials from the dc polarization curves. Fig. 8 shows an example of EIS spectra recorded on

Table 5
The apparent activation energy values calculated at several selected overpotentials for $SrRuO_3$ prepared by microwave assistant-citrate, citrate-nitrate and, coprecipitation methods.

Catalyst	E_a, kJ mol^{-1}					
	Equilibrium	−300 mV	−350 mV	−400 mV	−450 mV	−500 mV
$SrRuO_3$ (microwave)	6.67	13.75	13.89	16.16	17.38	19.22
$SrRuO_3$ (sol-combustion)	49.45	39.64	39.27	32.32	26.17	26.47
$SrRuO_3$ (coprecipitation)	86.32	51.37	50.88	43.92	39.01	36.90

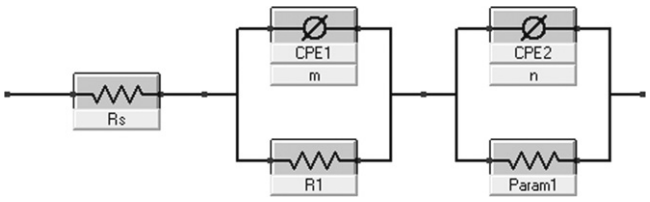

Fig. 9. Electrical equivalent circuit used to explain the EIS response of the HER on CpEs modified with $SrRuO_3$ prepared by different methods.

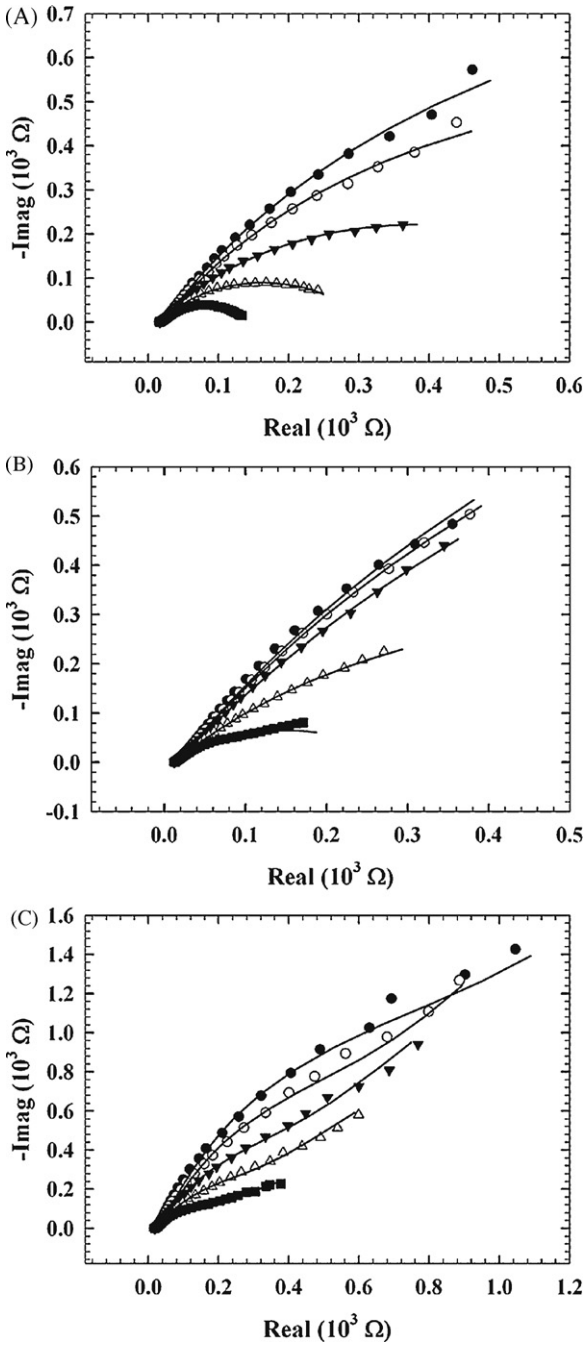

Fig. 10. Nyquist and Bode plots showing EIS response of CpE modified with 10% (w/w, %) $SrRuO_3$ prepared by (A) microwave assistant-citrate, (B) citrate-nitrate, (C) and coprecipitation methods in 0.1 M H_2SO_4 at various HER ovepotentials, symbols are experimental and solid lines are modeled data (−300 mV (●), −350 mV (○), −400 mV (▼), −450 mV (△), −500 mV (■)).

carbon paste electrode modified with 10% (w/w, %) $SrRuO_3$ prepared by microwave assistant-citrate method at overpotential of −0.1 V. The data are presented in the form of both (A) Bode and (B) Nyquist plots. The EIS spectra revealed the presence of two time constants. This was in agreement with EIS data obtained on other HER electrocatalysts [19,37]. In order to illustrate a physical picture of the electrode/electrolyte interface and the processes occurring at the electrode surface, experimental EIS data were modeled using non-linear least-squares fit analysis (NLLS) software and electrical equivalent circuit.

Fig. 8 shows that a very good agreement between the experimental (symbols) and simulated (lines) data are obtained when the equivalent circuit shown in Fig. 9 was used to describe the EIS response of the investigated catalyst. This model has been used o describe the response of the HER on porous electrodes [18,38,39]. It reflects the response of a HER system characterized by two time constants, only one of them (CPE1) is related to the kinetics of the HER, this time constant changes with overpotential. The second time constant (CPE2) is related to the porosity of the electrode surface, and does not change considerably with overpotential. Thus, in order to relate the two time constants to specific physical phenomena (charge-transfer kinetics, hydrogen adsorption, surface porosity), the dependence of each electrical equivalent circuit parameter on applied overpotential was investigated. Fig. 10A–C shows a set of EIS spectra recorded on carbon paste electrode modified with 10% (w/w, %) $SrRuO_3$ prepared by microwave assistant-citrate, citrate-nitrate, and coprecipitation methods, respectively at various overpotentials. The data in Figures demonstrated that the agreement between the experimental (symbols) and simulated (lines) data is very good at all the overpotentials investigated. The Figures show that the radius of the high-frequency semicircle (smaller semicircle) was potential-independent, it can be related to the electrode surface porosity response, while the radius of the low-frequency semicircle (larger semicircle) decreased with an increase in overpotential, was then related to the charge-transfer resistance process and double layer capacitance. Studies of the HER on solid electrodes [18,38,39] showed that when the radius of the high-frequency semicircle (smaller semicircle) is potential-independent, it can be related to the electrode surface porosity, while the potential-dependent low-frequency semicircle (larger semicircle) is then related to the charge-transfer resistance process and double layer capacitance. In such a case, a lower value time constant (high-frequency constant) represents a response of surface pores, while a higher value time constant (low-frequency constant) is related to the HER kinetics. Table 7a–c shows the electrical equivalent circuit parameters calculated from NLLS analysis for $SrRuO_3$ prepared by microwave assistant-citrate, citrate-nitrate, and coprecipitation methods, respectively. With an increase in overpotential, there are two important results: first CPE1 changed (decreased in case of $SrRuO_3$ prepared by microwave assistant-citrate and coprecipitation methods and increased in case of $SrRuO_3$ prepared by citrate-nitrate method) and R1 decreased correspondingly. It can be concluded that (CPE1-R1) was related to the HER charge-transfer kinetics, namely to the response of double layer capacitance characterized by CPE1 and HER charge-transfer resistance characterized by R1. The second result was in contrary to the behavior of CPE1, the value of CPE2 was shown change, but relatively in less constant. At the same time, the value of R2 decreased. This is a typical behavior related to the porosity of the electrode surface. A fitting procedure showed that a better agreement between theoretical and experimental data is obtained when pure capacitance was replaced by a frequency-dependent constant phase element, CPE. As already discussed before [39], the use of a CPE is required due to a distribution of the relaxation times as a result of non-homogeneities present at the micro- or nano- (atomic/molecular) level, such as

Table 7
The electrical equivalent circuit parameters calculated from the NLLS analysis for $SrRuO_3$ prepared by (a) microwave assistant-citrate, (b) citrate-nitrate and (c) coprecipitation methods.

η, V	*Rs*, $\Omega\,cm^2$	CPE1, $F\,cm^{-2}$	*m*	R1, $\Omega\,cm^2$	CPE2, $F\,cm^{-2}$	*n*	R2, $\Omega\,cm^2$
(a)							
−0.050	15.55	640.29	0.74	2276.91	253.81	0.49	8.03
−0.075	15.62	592.74	0.72	1613.09	305.31	0.51	6.72
−0.100	15.65	545.50	0.69	729.50	342.15	0.57	4.97
−0.125	15.54	596.79	0.71	284.39	388.29	0.53	5.84
−0.150	15.47	422.33	0.75	115.25	325.05	0.51	8.17
(b)							
−0.050	12.43	477.18	0.79	5.1	528.06	0.72	3808.78
−0.075	12.27	501.73	0.77	5.66	531.09	0.71	3480.16
−0.100	12.1	649.05	0.84	3.72	477.16	0.68	3509.9
−0.125	11.81	2136.89	1.24	0.69	364.01	0.60	1150.43
−0.150	12.69	4424.62	1.99	0.002	347.44	0.57	273.06
(c)							
−0.050	18.28	986.17	0.70	1.41×109	761.39	1.11	539.16
−0.075	18.08	992.97	0.69	1.59×106	607.57	1.13	271.69
−0.100	17.89	844.89	0.66	35841.18	594.82	1.10	158.00
−0.125	17.98	583.67	0.60	18132.33	711.60	1.01	129.01
−0.150	17.85	340.89	0.53	2324.12	1021.62	0.96	88.81

surface roughness/porosity, adsorption, diffusion, and non-uniform surface charge distribution.

This EIS behavior is quite in consistence with the Tafel behavior discussed previously. As from the Tafel measurements, the slow rate-determining step in the HER on the carbon paste electrodes modified with perovskites was the adsorption of hydrogen (Volmer), while the desorption step was fast. Consequently, the absence of an EIS hydrogen adsorption time constant could be expected, as also confirmed by the EIS measurements. This demonstrates that although EIS and Tafel techniques are two quite different experimental techniques, results obtained by both techniques are comparable.

4. Conclusion

$SrRuO_3$ was successfully prepared for the first time by the microwave assistant-citrate method. XRD data suggested the successful incorporation of Ru^{4+} at the Sr^{2+} cations sites confirming the formation of the orthorhombic perovskite phase of $SrRuO_3$ for all the prepared samples. $SrRuO_3$ prepared by the microwave synthesis provides the smallest particle size and the largest surface area and porosity compared to those prepared by the conventional chemical synthesis methods, namely citrate-nitrate and coprecipitation methods. Hence, it offers the highest catalytic activity toward HER. This was shown from the values of the exchange current density, the current density values at fixed overpotential of −300 mV and the overpotential values measured at current density of 1 $mA\,cm^{-2}$. The calculated values of the activation energy gave the same trend for catalytic activity. The reaction order values were found to be 1.14, 0.98, and 0.88 for $SrRuO_3$ prepared by the microwave, citrate-nitrate and coprecipitation methods, respectively. The fractional reaction order was expected for HER catalyzed by oxide catalysts. Both Tafel and the impedance data showed that the Volmer step is the rate-determining step.

Acknowledgement

We gratefully acknowledge the funding from Cairo University through the Vice President Office for Research Funds.

References

[1] W.R. Tinga, W.A.G. Voss, Microwave Power Engineering, Academic Press, New York, 1968.
[2] A.J. Berteaud, J.C. Badet, J. Microw. Power Electromagn. Energy 11 (1976) 315–320.
[3] N. Toshimaa, H. Yan, Y. Shiraishia, in: B. Corain, G. Schmid, N. Toshima (Eds.), Recent Progress in Bimetallic Nanoparticles: Their Preparation, Structures and Functions, Metal Nanoclusters in Catalysis and Materials Science, Elsevier, MO, USA; Oxford, United Kingdom, 2008, p. 49.
[4] M.P. Selvam, K. Rao, Adv. Mater. 12 (2000) 1621–1624.
[5] K.E. Gibbons, S.J. Blundell, A.I. Mihut, I. Gameson, P.P. Edwards, Y. Miyazaki, N.C. Hyatt, M.O. Jones, A. Porch, Chem. Commun. 1 (2000) 159–160.
[6] M.P. Selvam, K.J. Rao, J. Mater. Chem. 13 (2003) 596–601.
[7] H. Yan, X. Huang, Z. Lu, H. Hu, R. Xue, L. Chen, J. Power Sources 68 (1997) 530– 532.
[8] Z. Kowalczyk, S. Jodzis, N. Rarog, J. Zielinski, J. Pielaszek, Appl. Catal. A 173 (1998) 153–160.
[9] N.K. Labhsetwar, V. Balek, E. Večerníková, P. Bezdička, J. Subrt, T. Mitsuhashi, S. Kagne, S. Rayalu, H. Haneda, J. Colloid Interface Sci. 30 (2006) 232–236.
[10] B.D. Cullity, Elements of X-ray Diffraction, 2nd ed., Addision Wealey Pub. Company, USA, 1978.
[11] A. Damian, S. Omanovic, J. Power Sources 158 (2006) 464–476.
[12] K.R. Christmann, in: Z. Poal, P.G. Menon (Eds.), Hydrogen Effects in Catalysis, Marcel-Dekker, 1988.
[13] J.G. Highfield, K. Oguro, B. Grushko, Electrochim. Acta 47 (2001) 465–481.
[14] A. Rami, A. Lasia, J. Appl. Electrochem. 22 (1992) 376–382.
[15] N. Krstajic, S. Trasatti, J. Appl. Electrochem. 28 (1998) 1291–1297.
[16] C.A. Marozzi, A.C. Chialvo, Electrochim. Acta 46 (2001) 861–866.
[17] Southampton Electrochemistry Group, Instrumental Methods in Electrochemistry, Wiley, New York, 1985.
[18] B. Borresen, G. Hagen, R. Tunold, Electrochim. Acta 47 (2002) 1819–1827.
[19] E. Ndzebet, O. Savadogo, Int. J. Hydrogen Energy 20 (1995) 635–640.
[20] J.G. Highfield, E. Claude, K. Oguro, Electrochim. Acta 44 (1999) 2805–2814.
[21] R. Simpraga, G. Tremiliosi-Filho, S.Y. Qian, B.E. Conway, J. Electroanal. Chem. 424 (1997) 141–151.
[22] M. Siswana, K.I. Ozoemena, T. Nyokong, Talanta 69 (2006) 1136–1142.
[23] M. Ghiaci, B. Rezaei, R.J. Kalbasi, Talanta 73 (2007) 37–45.
[24] P. Ahonen, A.S. Gurav, E.I. Kauppinen, M.J. Hampden-Smith, T.T. Kodas, J. Aerosol Sci. 27 (1996) 373–374.
[25] T.-S. Hyuna, H.-G. Kimb, I.-D. Kima, J. Power Sources 195 (2010) 1522–1528.
[26] E. Fachinotti, E. Guerrini, A.C. Tavares, S. Tasatti, J. Electroanal. Chem. 600 (2007) 103–112.
[27] H. Inoue, J.X. Wang, K. Sasaki, R.R. Adzic, J. Electroanal. Chem. 554–555 (2003) 77–85.
[28] A. Qi, S. Wang, G. Fu, C. Ni, D. Wu, Appl. Catal. A 281 (2005) 233–246.
[29] B.E. Conway, in: A. Wieckowski (Ed.), Interfacial Electrochemistry, Marcel-Dekker, New York, 1999.
[30] N. Krastajic, M. Popovic, B. Grgur, M. Vojnovic, D.J. Sepa, J. Electroanal. Chem. 512 (2001) 27–35.
[31] E. Ndzebet, O. Savadogo, Int. J. Hydrogen Energy 26 (2001) 213–218.
[32] M.J. Giz, S.A.S. Machado, L.A. Avaca, E.R. Gonzalez, J. Appl. Electrochem. 22 (1992) 973–977.
[33] M.J. Giz, S.C. Bento, E.R. Conzalez, Int. J. Hydrogen Energy 25 (2000) 621–626.
[34] D.B. Sepa, in: J.O.M. Bockris, B.E. Conway, R.E. White (Eds.), Modern Aspects of Electrochemistry, vol. 29, Plenum Press, New York, 1996, p. 10.
[35] M.J. Giz, G. Tremiliosi-Filho, E.R. Conzalez, Electrochim. Acta 39 (1994) 1775–1779.
[36] H.J. Miao, D.L. Piron, Electrochim. Acta 38 (1993) 1079–1085.
[37] E. Navarro-Flores, Z. Chong, S. Omanovic, J. Mol. Catal. A: Chem. 226 (2005) 179–197.
[38] B. Losiewicz, A. Budniok, E. Rowinski, E. Lagiewka, A. Lasia, Int. J. Hydrogen Energy 29 (2004) 145–157.
[39] L. Birry, A. Lasia, J. Appl. Electrochem. 34 (2004) 735–749.